

## THE REFINEMENT OF GEOMORPHOLOGICAL AND GEOCHEMICAL STATISTICAL TECHNIQUES IN THE STUDY OF CLAY-BASIN TECTONICS: THE ERA BASIN (CENTRAL ITALY)

G. Ciotoli<sup>(3)</sup> - S. Lombardi<sup>(1)</sup> - S. Serafini<sup>(2)</sup> - F. Zarlenga<sup>(2)</sup>

<sup>(1)</sup>Dept. of Earth Sciences, University of Rome "La Sapienza", Roma, Italy

<sup>(2)</sup>ENEA/CRE-Casaccia, Dept. of Environment, Roma, Italy

<sup>(3)</sup>Research Doctorate c/o Dept. of Earth Sciences, University of Rome "La Sapienza", Roma, Italy

**RIASSUNTO** - *Affinamento di metodologie statistiche geochimiche e geomorfologiche per lo studio della tettonica di un bacino argilloso: il bacino di Era (Italia centrale)* - Il Quaternario *Italian Journal of Quaternary Sciences*, 10(2), 1996, 231-246 - In questo lavoro viene presentata una nuova metodologia di indagine volta agli studi di neotettonica nei bacini argillosi e basata sull'integrazione di dati geochimici, morfologici e strutturali. I dati geochimici si riferiscono alle analisi delle concentrazioni di elio in 919 campioni di gas del suolo. Il campionamento è stato effettuato nella val d'Era uno dei bacini argillosi neogenici del settore peritirrenico dell'Italia centrale (Toscana). La distribuzione delle concentrazioni dei gas nel suolo è stata confrontata con l'ubicazione e l'orientazione della tettonica fragile (faglie e fratture) tratte dalla letteratura e da indagini di campagna (analisi mesostrutturale), e con le caratteristiche morfotettoniche ottenute tramite fotointerpretazione ed analisi del reticolo di drenaggio superficiale. I dati ottenuti sono stati trattati statisticamente e confrontati mediante diagrammi stellari. Sia l'approccio statistico sia l'associazione della distribuzione spaziale delle anomalie geochimiche con gli elementi morfologici e strutturali messi in evidenza dalle analisi di campagna mostrano che le direzioni più rappresentative sono NW-SE e SW-NE, in accordo con i ben noti trends strutturali appenninici ed anti-appenninici del settore di catena. Inoltre, le anomalie di elio nei gas del suolo che mostrano un trend N-S ed E-W sono probabilmente da attribuire ad una fase deformativa più recente che agisce tuttora in queste direzioni. Questa ipotesi viene rafforzata dalla buona corrispondenza, sia a scala regionale che a scala locale (settori nei pressi degli abitati di Peccioli e di Orciatice-Montecatini in Val di Cecina), tra i dati geochimici ed i risultati delle analisi strutturali e geomorfologiche. La tecnica dei gas del suolo si mostra essere un valido mezzo esplorativo per gli studi di neotettonica nell'individuazione di faglie e/o fratture soprattutto nei bacini argillosi dove la presenza di elementi di tettonica fragile può essere mascherata dalle caratteristiche tecniche (plasticità) e dallo spessore elevato dei sedimenti.

**ABSTRACT** - *The refinement of geomorphological and geochemical statistical techniques in the study of clay-basin tectonics: the Era basin (Central Italy)* - Il Quaternario *Italian Journal of Quaternary Sciences*, 10(2), 1996, 231-246 - A comparative approach to neotectonic studies is presented, which encompasses the integration of geochemical, morphological and structural analyses. Nine-hundred-nineteen soil gas samples were collected in the Era basin (Tuscany, Central Italy) and their helium contents were measured. Helium distribution has been compared with location and orientation of known brittle deformations (faults and fractures) and morphological features obtained by air-photo interpretation and drainage network analyses. Obtained data were statistically compared by means of rose diagram plots concerning the investigated parameters and locally studied by associating the observed helium anomaly ridges with the known morphological and structural elements. The statistical approach showed a good convergence between the applied methodologies. Data from geomorphological, mesostructure, and geochemical surveys are consistent with the NE-SW and NW-SE orientations, i.e. Apennine and anti-Apennine trend of the known structural pattern. Moreover the apparent N-S and E-W trending helium anomalies are thought to be due to the Middle Pleistocene deformation phase along these directions. The relationship between helium distribution and the strain field is strengthened by the good correspondence, at local scale, among geochemical data and results of the structural and geomorphological features (Orciatice-Montecatini Val di Cecina and Peccioli areas). However helium soil gas technique showed to be a sensible tool for neotectonic studies in clay basin, as soil gas defines the leakage of deep seated gas along tectonic discontinuities even if they have no surface evidence and where the clay deposit is hundreds of meters thick.

**Keywords:** Neotectonics, soil gas, photolineaments, drainage network, mesostructure analysis

**Parole chiave:** Neotettonica, gas del suolo, fotolineamenti, reticolo idrografico, analisi mesostrutturale

### 1. INTRODUCTION

Earth degassing is the process whereby deep-origin gases migrate to the soil surface through the mantle and the crust. The measure of the concentration of these naturally occurring gases in the soil has been shown to be a useful method for the detection of faults and fracture systems which act as preferential pathways for the ascent of deep gases (Gregory & Durrance, 1985; Duddridge *et al.*, 1991).

Recent field data indicate the reliability of soil-gas method for detecting buried structural discontinuities also in areas characterised by non-cohesive sediments where the mapping of tectonic discontinuities by direct methods is made difficult by the plastic behaviour of the sedimen-

tary cover (Lombardi *et al.*, 1993; 1996; Durrance & Gregory, 1988; Etiope, 1995).

Generally, atmosphere and soil air can be considered to have similar gas concentration which can be referred to a background value. It is possible, however, to measure gas values in the soil that are very different from those in the atmosphere (soil-gas anomalies). In particular this phenomenon may happen in correspondence with faults and fractures whereby endogenous gases are transported to the soil. In these zones the soil gas distribution shows higher values than the background atmospheric values, and the shape of these anomalous concentrations generally reflect the location and the direction of gas conduits (faults). This observation represents the basic idea behind the application of

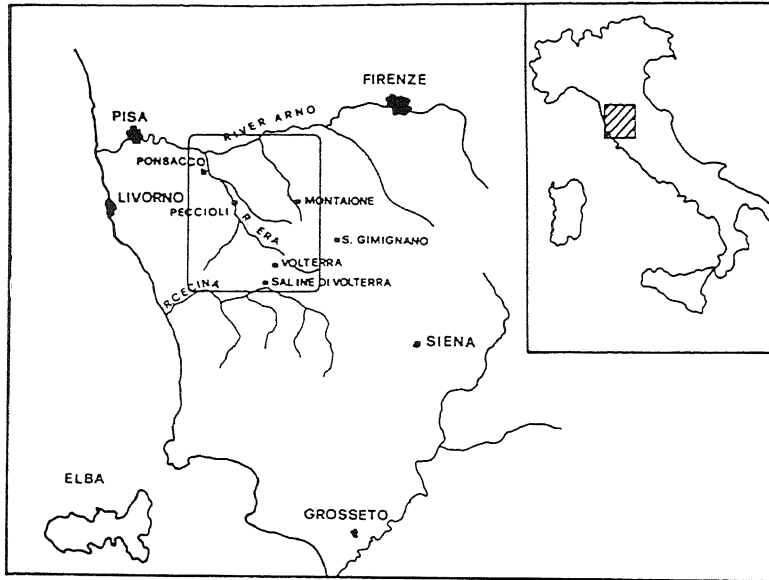


Fig. 1 - Key map of the surveyed area.  
Localizzazione geografica dell'area di indagine.

soil-gas method for tectonic prospecting (Wakita *et al.*, 1980; Zhiguan, 1991; Ciotoli *et al.*, 1993; Klusman, 1993), and its rapidity and low-cost make this method a powerful tool for geological investigation.

Soil-gas distribution can, nevertheless, be affected by surface features such as pedological, biogenic and meteorological factors; however, these factors are supposed to have a subordinate effect on gas leakage to deep fault-related features. Hence, it is necessary to collect a large number of samples during periods of stable meteorological conditions (*i.e.* during dry season), and use an appropriate statistical treatment.

The distribution of soil-gas helium and geo-structural data (obtained by statistical analysis of lineaments from aerial photos, analysis of stream segments and field-based structural mapping) has been compared in the Val d'Era clayey basin (Tuscany, Central Italy) as an example of the utility of such an approach to better understand the presence and influence of buried structures on gas migration and concentration in the subsurface.

The goal of this work is to give a useful contribution to the detection of tectonic discontinuities whose presence had only been suggested by indirect stratigraphic and morphological evidence.

Each of these techniques has been applied in tectonic studies, however the comparison of two or more of above methods have seldom been attempted. The proposed integrated approach may be of interest for the study of regional tectonics in clayey basins for several reasons: (i) geological and geophysical surveys, usually applied in tectonic research, may fail when applied in clayey basins due to the physical and mechanical characteristics of clay and (ii) its low cost relative to the cost of more traditional studies, especially geophysics.

## 2. THEORETICAL PRINCIPLES

The use of deep-seated gases in soil air as fault

and fracture tracers has been proposed by several authors since 1930 (Illing, 1933; Muskat, 1946), as the presence of endogenous gases in soil air can be linked to their ascent along fault and fracture systems which act as preferential migration pathways (Duddridge *et al.*, 1991; Lombardi & Reimer, 1990; Reimer, 1990).

Among the terrestrial gases helium for its mantle and/or deep crust origin has been shown to be one of the most reliable geochemical pathfinders, particularly as a tracer of deep gas-bearing faults.

As a fracture tracer  $^4\text{He}$  has many distinctive features: being chemically inert, physically stable, sparingly soluble in water and practically unabsorbable it is one of the most mobile elements; furthermore it is definite by of deep origin because 97% of helium is produced below the sedimentary cover (Pogorsky & Quirt, 1981).

Helium has two stable isotopes:  $^3\text{He}$  (primordial) from mantle degassing and  $^4\text{He}$ , produced by "alfa" decay of the uranium and thorium series accumulated in the metamorphic basement, geothermal fluids, uraniferous ore and petroleum reservoirs, etc. Since the latter represents almost 100% of total helium, gas collected from soil is essentially  $^4\text{He}$  (Oliver *et al.*, 1984).

From soil helium disperses into the atmosphere where, owing to a dynamic equilibrium, it has a constant concentration of  $5220 \pm 15\text{ppb}$  (Holland & Emerson, 1990). This concentration is considered as a reference standard, and thus in the following discussion results are expressed in ppb (v/v) as the difference ( $\Delta\text{He}$ ) between sample and atmospheric helium concentrations.

Some authors (Gregory & Durrance, 1985) suggest that the presence of fracture systems may be indicated by either positive or negative helium anomalies, depending on near-surface conditions. Positive helium anomalies occur in dry soil where fractures act as high permeability migration pathways while negative or near-zero anomalies suggest zones characterised by the presence of moisture and good soil aeration or zones where the fractures are water-conducting; in the latter case gas depletion occurs due to the low solubility of helium in water.

The interpretation of the relationship between structural and geochemical data may be, moreover, affected by sampling strategy in that the sampling density used may cause the loss of some information and by the different permeability of fracture systems due to different age of activation and/or self-sealing phenomena. Nevertheless soil-gas surveys have proven to be useful tool in detecting fracture and fault systems, even in sedimentary basins where Plio-Pleistocene clay fill may mask the surface expression of structural features.

In general soil-gas anomalies are significantly different from the air concentration values. In this way a preliminary qualitative definition of "anomalous value" is provided. Yet, in order to better assess the "tectonic" meaning of an anomalous value (*i.e.* an upward migration along a gas-bearing fault) and to permit its definition two aspects have to be considered:

- instrumental sensitivity;
- the geometrical shape of the anomalies.

The first aspect concerns the general sampling and analytical methods. The second aspect suggests a "geometric" meaning of "anomaly". Linear anomalies frequently occur in soil-gas concentration maps, which are often taken as a strong proof of tectonic control of gas migrating along gas-bearing fractures (Fridman, 1990). It is unlikely that linear anomalies longer than several meters can be due to biological and meteorological effects, or to sampling and analytical errors.

Now the problem is to define the value beyond which samples have to be considered as anomalous. Generally, all geochemical data are characterised by high variability, therefore is quite difficult to establish if a measured gas concentration has to be considered as a natural anomaly (outliers) or as a methodological error (sampling and analytical conditions). The very common practice to consider the mean plus 'n' times the standard deviation as being anomalous is not formally correct, because of a non-normal frequency distribution of sample set (Davis, 1986). Nevertheless this procedure was followed, being generally accepted in soil-gas interpretation (McCarthy & Reimer, 1986; Klusman, 1993; King *et al.*, 1996; Vakin & Lyalin, 1990) and convenient for comparison with previous surveys. Furthermore, as the presence of a few outliers may often provide non-representative statistical parameters, gas values greater than 95th percentile and lower than 5th percentile were excluded. The mean and the standard deviation of the corrected data set were used to define the statistical anomaly threshold fixed at the mean plus 1/2 standard deviation. Generally, this anomaly threshold agree with that calculated following Lepeltier (1969), which are obtained from the change in slope of the cumulative frequency distribution plot.

### 3. STATISTICAL ANALYSIS OF RECTILINEAR STREAM SEGMENTS

This analysis identifies possible correlation between the average orientation of rectilinear stream segments and that of the fracture systems. Analogous, statistically-based research, has highlighted the often complex connection between these two features (Cosentino *et al.*, 1987; Ciccacci *et al.*, 1987; Scheiddegger, 1980; 1981), as the development of the drainage network is controlled not only by the morphology and lithology, but also by structural features. Analysis was performed by digitizing the drainage network on 1:25,000 scale topographic maps, by the "Territorial Information System E.L.I.S.A." on an Apollo DN 4000 work station of ENEA/Casaccia Data Processing Center, and processing the resultant data with the software package "Statview".

### 4. STATISTICAL ANALYSIS OF LINEAMENTS

The interpretation of lineaments from satellite images (ERTS, LANDSAT, SPOT) or side illuminated relief maps ("shadow method") is not unequivocal, as suggested by Salvini (1993) and Wise *et al.* (1985). Many authors

(Bagheri & Kiefer, 1986; Galadini & Salvi, 1990) have adopted the "lineament" definition of O'Leary *et al.*, (1976), while a similar geomorphological definition has been proposed in Italy (Carraro *et al.*, 1978; Gruppo di Geol. Spaziale del Settore Alpino, 1978). In the most recent works it appears possible to directly confirm some lineaments with geological mapping (Bemporad *et al.*, 1986; Bollettinari & Mantovani, 1986; Frezzotti & Giraudi, 1986; Galadini & Salvi, 1990). Some authors suggest that a correspondence between geological features and lineaments can only be defined if a large representative number of lineaments are analysed statistically and represented through rose diagrams and density distribution maps (Al Fasatwi & Van Dijk, 1990; Chorowicz *et al.*, 1991; Danielska *et al.*, 1986; Defu *et al.*, 1986; Elsinga & Verstappen, 1989; Kibitlewski & Danielska, 1986), while others suggest integrating their results with a mesostructural survey (Karpuz *et al.*, 1993; Zanchi & Tozzi, 1987). Recent approaches include varying the luminance signal in some direction around an image point (Le Corre & Quete, 1993); integrating geophysical, digital-elevation and geological data sets (Karpuz *et al.*, 1993; Stefouli & Angelopoulos, 1990), and enhancing linear features by filtering in Fourier space (Nino *et al.*, 1993).

In comparison with satellite images the interpretation of aerial photographs is still largely and successfully employed, often with economic advantage, in many applications of geological survey. Photo-interpretation offers the advantage directly defining the landforms of probable tectonic origin (Brancaccio *et al.*, 1986; Pa-nizza, 1988; Perotti *et al.*, 1988) (Table 1). It is worth noting that some authors also suggest a field check for each lineament (Castaldini & Panizza, 1988; Panizza *et al.*, 1987), in particular for those caused by "geomorphological con-

Table 1 - Morphosculptures of possible neotectonic origin obtained from the analysis of aerial photo-lineaments.

*Morfosculture di probabile origine tettonica evidenziate dall'analisi fotogeologica.*

RIDGES	<ul style="list-style-type: none"> <li>- Planoaltimetric and altimetric variations of ridge lines</li> <li>- Saddle alignments</li> </ul>
SLOPES	<ul style="list-style-type: none"> <li>- Escarpments</li> <li>- Triangular, trapezoidal and/or pentagonal facets related to the fluvial erosion</li> <li>- Rectilinear slopes</li> </ul>
VALLEYS	<ul style="list-style-type: none"> <li>- Rectilinear stream segments</li> <li>- Transverse scarps in river beds</li> <li>- Rectilinear valley</li> <li>- Sharp bends in river beds</li> <li>- Upstream river confluences</li> </ul>

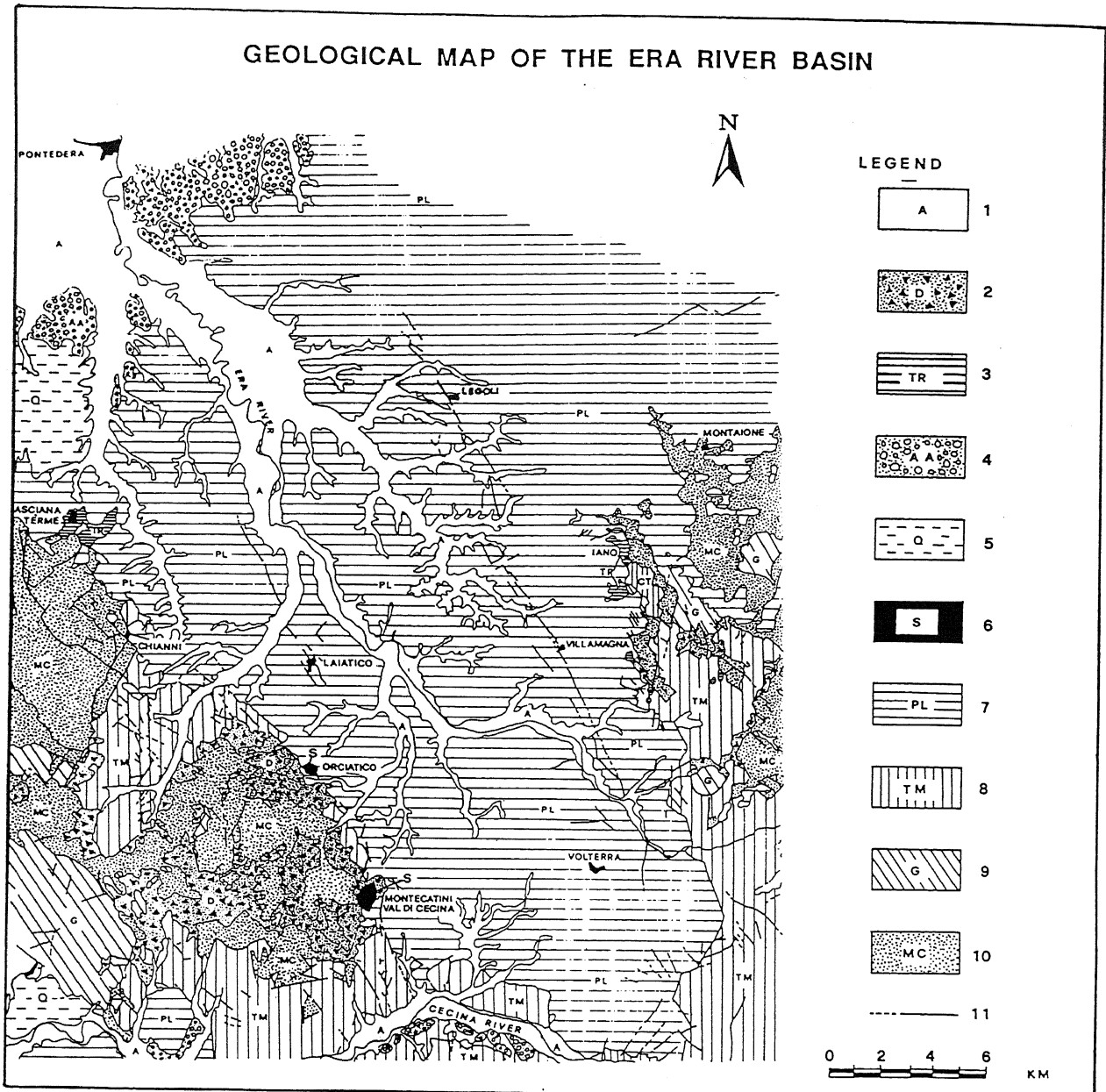


Fig. 2 - Geological sketch map of the Era river basin. Legend: 1) valley bottom recent alluvial deposits; 2) slope debris; 3) travertines (Holocene); 4) ancient alluvial deposits (Lower Pleistocene); 5) clay and sands (Lower Pleistocene); 6) trachyte intrusive body (Middle Pliocene); 7) clay, sand and conglomerates (Lower Pliocene); 8) clay, sand and conglomerates (Messinian); 9) gabbro, serpentine and diabase (Malm); 10) Carboniferous and Meso-Cenozoic rocks; 11) faults (dashed if supposed).

*Schema geologico del bacino del fiume Era. Legenda: 1) alluvioni recenti di fondovalle; 2) corpi in frana; 3) travertini (Olocene); 4) alluvioni antiche (Pleistocene inferiore); 5) argille e sabbie (Pleistocene inferiore); 6) intrusione di trachite (Pliocene medio); 7) argille, sabbie e conglomerati (Pliocene inferiore); 8) argille, sabbie e conglomerati (Messiniano); 9) gabbri, serpentini e diabasi (Malm); 10) rocce carbonifere e meso-cenozoiche; 11) faglie (a tratteggio se supposte).*

vergence" (Brancaccio *et al.*, 1986; Panizza & Piacente, 1988; Verstappen, 1983). In this work aerial photographs were analysed for morpho-structure alignments of neotectonic significance. The chosen lineaments were processed statistically and then this data base was integrated with a mesostructural survey, as already experimented by Cosentino *et al.* (1987) and Zarlenga (1985) in areas characterised by different geological settings.

## 5. MESOSTRUCTURAL ANALYSIS

Mesostructural analysis consists in statistically processing a collection of structural elements (Davis, 1984). In this work only meso-scale brittle deformations were processed, with subsequent interpretation based on both theoretical and empirical models (Cloos, 1986; Stearns *et al.*, 1981). The adopted method is similar to that described in Salvini & Vittori (1982) and consists in the

field collection of structural elements (normal and reverse faults, fractures, etc.) which are digitised and inserted into a data base for being subsequently computer-processed. This processing defines polymodal distributions using a statistical-geometric method based on the Schmidt projection (lower hemisphere) (Ragan, 1967), with clustered distributions suggesting the orientation of principal stress axes ( $\sigma_1$ ,  $\sigma_2$ ,  $\sigma_3$ ). According to the Anderson's (1951) dynamic classification of faults, because no shearing stress can exist at the Earth's surface, for a surface faulting mechanism one of the principal stress axes must be perpendicular to the Earth's surface. In order to decrease localised effects this approximation seems to be acceptable for surface brittle deformations statistically elaborated

(Serafini & Vittori, 1986) with Fortran code on an OH 4150 computer at ENEA/DISP Data Processing Centre.

## 6. GEOLOGICAL AND STRUCTURAL BACKGROUND OF THE ERA RIVER BASIN

The Era River basin, which covers an area of 591 km<sup>2</sup> along the Tyrrhenian margin of central Italy (Fig. 1) (Boccaletti *et al.*, 1990), began to form during the Upper Tortonian. The extensional tectonic movements which occurred in Tuscany and Latium during this period reached their maximum during the Lower Pliocene (Ambrosetti *et al.*, 1978; Ber-tagnini *et al.*, 1991; Boccaletti & Coli, 1983), with

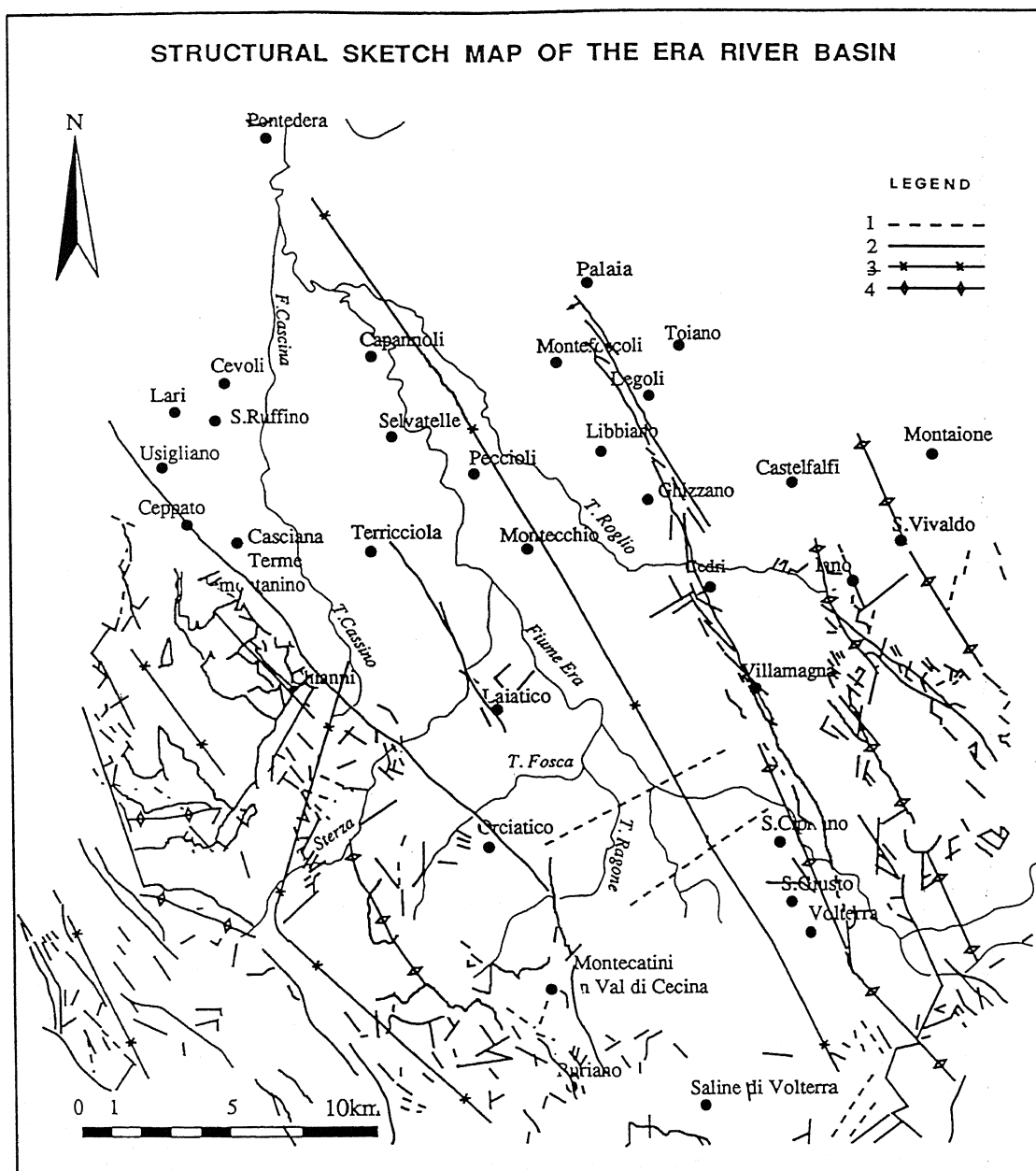


Fig. 3 - Structural sketch map of the Era river basin: (1) supposed faults; (2) known faults; (3) synclinal axis; (4) anticlinal axis.  
 Schema strutturale della Val d' Era: (1) faglie presunte; (2) faglie certe; (3) assi di sinclinale; (4) assi di anticlinale.

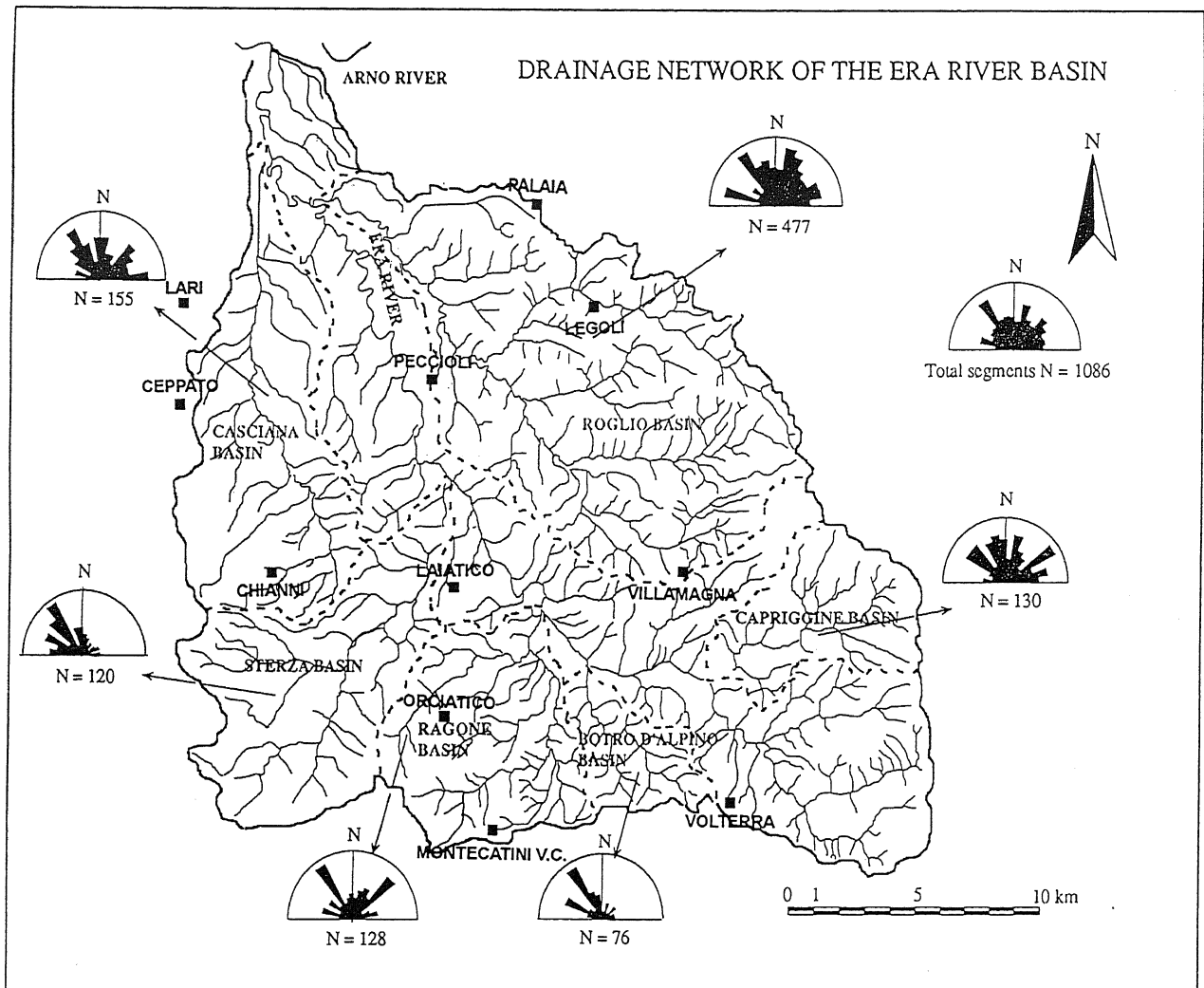


Fig. 4 - Drainage network sketch map and rose diagrams showing the directions of linear fluvial segments >250 m related to the minor basins of rivers tributary of the Era river.

Carta del reticolo idrografico del bacino del fiume Era. I diagrammi semipolari mostrano l'orientazione statistica dei tratti fluviali rettilinei maggiori di 250 m relativi ai bacini minori.

associated block faulting forming a series of NW-SE trending structural lows, which would be filled by Neogene sediments, and ridges (structural highs) where the substratum outcrops. Towards the east, the Era River basin is bounded by the faulted northern sector of the "Middle Tuscan Ridge" (Fig. 2).

In the western side of the Era valley the basin is bordered by the Casciana Terme-Chianni structural high where the Tuscan nappe (from Lower Lias) and allochthonous Ligurid Units, as well as the semi-allochthonous successions ("Alberese Formation"), and neo-autochthonous cycles, outcrop (Mazzanti *et al.*, 1963; Squarci & Taffi, 1963). In the south-western part of the basin, trachite intrusions (4.1 Ma B.P.) (Ferrara *et al.*, 1988) intersect the basement as well as the Pliocene formations near Montecatini in Val di Cecina and Orciatice.

The Recent series are more than 1000 m thick and consist of sediments deposited during the Upper Miocene after the collapse of the pre-Neogene basement. During this period initial lacustrine sedimentation (conglomerates, sands and clays) was followed by marine deposi-

tion (clastic, organogen and evaporite deposits). Subsequently, during the Middle-Lower Pliocene, some sectors underwent further subsidence and sedimentation increased (clays, sands, conglomerates and limestones with *Amphistegina*) whereas stable zones remained above sea level (Dallan *et al.*, 1969). The Era valley was subjected to uplift during the Upper Pliocene which resulted in emersion and tilting toward the N and NW, probably caused by normal faults localised at the foot of Mt. Pisano (Mazzanti, 1983) and now buried by the Arno River fluvial deposits. During the lower Pleistocene the sea flooded the southern part of the basin and this region did not re-emerge until the Sicilian (Mazzanti *et al.*, 1963). On the eastern side of the Era Valley (Fig. 3), Mazzanti (1961) recognised the NW-SE trending Legoli-Villamagna fault line, which are linked by a limited number of NE-SW trending normal faults.

On the western side of the valley, in the Chianni-Laiatico-Orciatice area, anti-Appennine (NE-SW trending) faults are linked to the tectonics of the neo-autochthonous cycle and are displaced by transverse faults

(Squarci & Taffi 1963). In the southernmost sector of the basin the faults are preferentially oriented N-S. The south-western border of the Era river basin is characterized by NW-SE trending boundary faults; these discontinuities provide ascent pathways for the Orciatice trachyte. This fault system is displaced in the northern sector by E-W trending faults.

Two main fault systems have been recognized between Montecatini in Val di Cecina and Orciatice, which trend NW-SE (locally N-S) and E-W (Mazzanti *et al.*, 1963). The normal fault systems, which trend NW-SE (N20°-40°W) and N-S, are considered to have been active from the Lower Pliocene to the Middle Pleistocene, while the NE-SW fault system was active only from the Upper Pliocene to the Lower Pleistocene.

Many thermal and mineral springs upwell in the lateral parts of the basin and are connected with faults which intersect the basement formations. Southward, the Era River basin borders the geothermal area of Larderello.

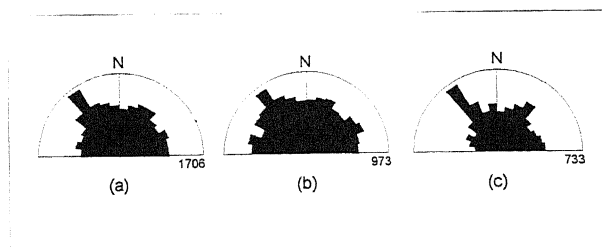


Fig. 5 - (a) Rose diagram of the distribution of the directions of the whole set of chosen segments in the Era basin (1706 elements), (b) rose diagram of the right effluents of the Era river, (c) rose diagram of the left effluents of the Era river.

(a) Diagramma semipolare relativo alla distribuzione della direzione dell'intero set delle aste fluviali rettificate (1706 elementi), (b) diagramma relativo agli affluenti di destra, (c) diagramma relativo agli affluenti di sinistra.

## 7. RESULTS

### 7.1 Statistical analysis of rectilinear stream segments

The drainage network was first traced (Fig. 4) from topographic maps (scale 1:25,000) and aerial photographs then rectified with a semiautomatic digitizing process. As recommended by Cosentino *et al.* (1987), only the rectilinear segments longer than 1 cm on the map (250 m) were considered, excluding streams with alluvial bottom valley deposits, and only tributary basins of the Era River were distinguished. Further discrimination of minor stream orders, as outlined in Bisci *et al.* (1988) and Ciccacci *et al.* (1987), was not adopted because it does not yield sufficient minor river-basins segments for reliable statistical analysis. Data were represented with rose diagrams that show the preferential direction of linear fluvial segments.

A total of 1706 linear elements were defined and stored in a data base. Results show (Fig. 5a) that the water courses are preferentially orientated parallel to an Apennine trend of N30°-40°W, with little apparent differences between the right and left watercourses of the Era river (Figs. 5b and 5c).

Analysis of minor tributary streams (Fig. 4) shows

the following trends for the right effluents:

- "Botro dell'Alpino" basin N30°-40°W and N60°-70°W;
- "Roglio" basin N20°-30°E, N30°-40°W and N70°-80°W;
- "Capriggine" basin N50°-60°E, N50°-70°W, N10°-20°E, N10°-20°W.

For the left effluents the trends are:

- "Sterza" basin N30°-40°W;
- "Ragone-Fosce" basin N30°-40°W and N40°-50°E;
- "Casciana" basin N30°-40°W, N-S, N40°-50°E, and E-W.

Rose diagrams show that the N-S trend is more common in northern basins (Sterza, Roglio and Casciana basins) than in the southernmost basins.

### 7.2 Statistical analysis of aerial photo lineaments

Interpretation of 1:33,000 scale aerial photograph (GAI Flight, 1954) consisted of the identification and selection of alignments likely formed by neotectonics (Table 1), which were subsequently transferred to a small-scale topographic map (Fig. 6). As a field check was not performed for each lineament, the features have been statistically processed. The resultant rose diagram (Fig. 7a) shows three main trends: Apennine N30°-40°W (44 elements), anti-Apennine N20°-30°E (29 elements) and N10°W (18 elements). By comparing this diagram to the rose diagram (Fig. 7b) relative to known faults of the Era River basin, a number of common peaks are evident: N30°-40°W (52 elements), N-S (46 elements) and a minor peak N20°-30°E (39 elements).

### 7.3 Statistical analysis of brittle deformations

Mesostructural analysis was performed on 51 stations, including a total of 638 measured elements; their distribution is not homogeneous due to the lack of outcrops. The surveyed sediments are exclusively Lower Pliocene to Quaternary in age. Structural data (azimuth and dip) were graphically and statistically processed for each station and fault and fracture planes are projected on a Schmidt net (Fig. 8). Figure 9 (a, b) shows the rose diagrams relative to fracture and fault orientations, respectively. In general there is good agreement between fault and fracture trends, including an Apennine (N20°-50°W), an anti-Apennine (N20°-50°E) and a weak N-S trend.

### 7.4 Helium distribution in soil gas

The soil-gas survey was performed within the summer months during a period of stable meteorological conditions. A total of 919 soil gas samples were collected and analysed from an area of about 600 km<sup>2</sup> (about 1.5 samples/km<sup>2</sup>) using well-established techniques (Reimer, 1990; Lombardi & Reimer, 1990). In brief the method is as follows. First an 8 mm-diameter hollow steel probe is driven into the ground to a depth of 50 cm. The probe is purged and 50 cm<sup>3</sup> of soil gas are extracted with a syringe and transferred for storage and future analysis into a pre-evacuated stainless steel cylinder. The helium content was determined by a mass spectrometer (VARIAN Leak Detector 938-41) having an instrumental error of about 20 ppb. Gas data were computer processed to

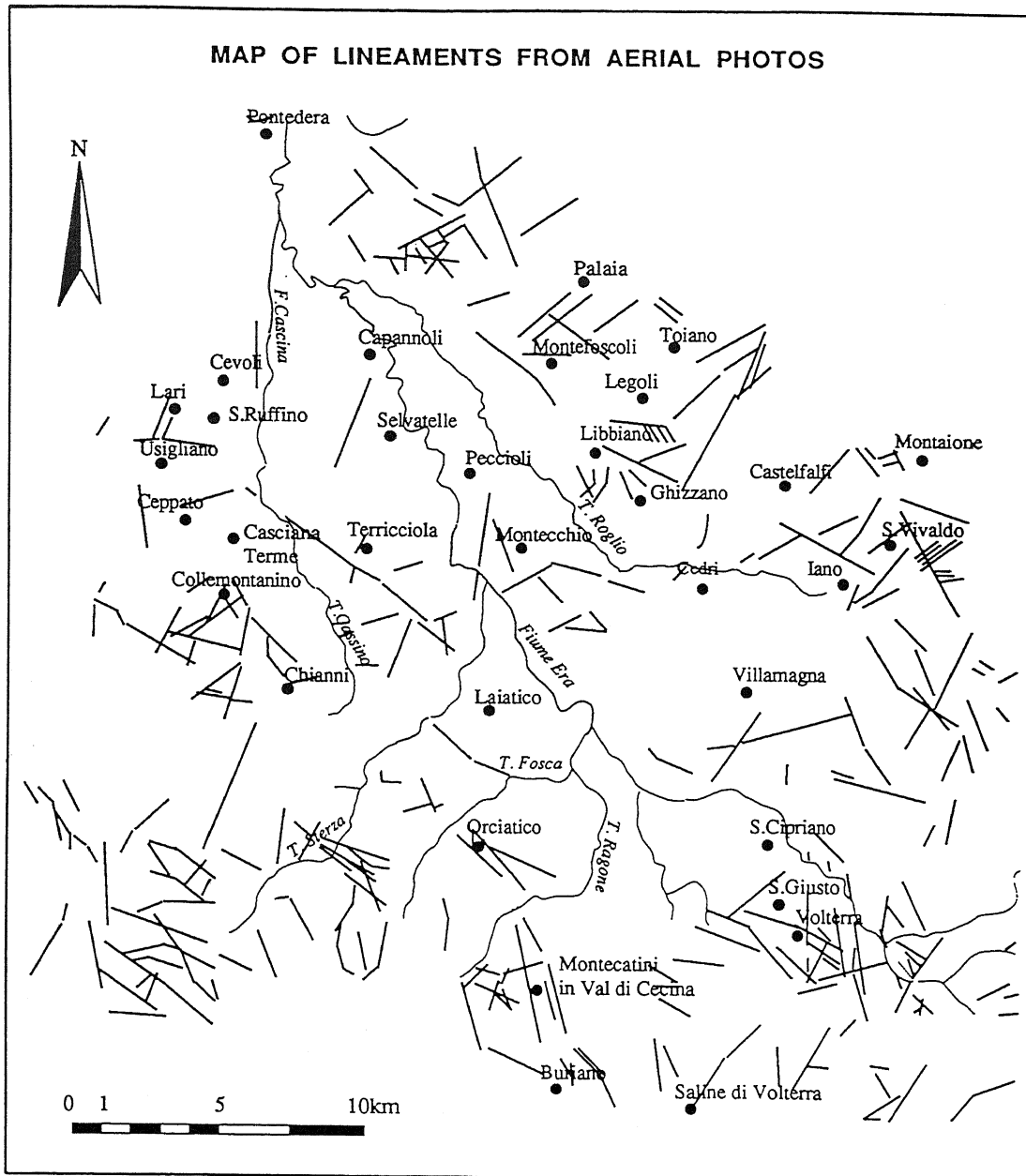


Fig. 6 - Map of lineaments from aerial photographs.  
*Carta dei lineamenti derivati da foto aeree.*

produce dot-maps. Helium statistics are summarised in Table 2.

By excluding the values greater than 95th percentile and lower than 5th percentile, the resulting  $\Delta\text{He}$  average value is 212 ppb. Anomalous helium concentrations, above the mean value plus 1/2 standard deviation ( $\Delta\text{He} > 262$  ppb), are about 36% of the whole data set. Previous surveys carried out in other Neogene clay basins in Italy have provided background values ranging between 0 and 200 ppb (Lombardi *et al.*, 1993; 1996). Negative values of  $\Delta\text{He}$  (only about 4% in this work) were found to occur widely in soil gas investigations, also in correspondence of faults (Klusman, 1993; Gregory & Durrance, 1985; Bertrami *et al.*, 1984), and are thought to be due to disequilibrium between soil gas and the atmosphere and/or to water saturated terrains. The steps in the fre-

quency distribution histogram highlight the presence of two threshold values of 130 ppb and 290 ppb defining samples near the atmospheric helium content (negative to 130 ppb), the background concentrations (130-290 ppb) and the anomalous values (up to 290 ppb) respectively (Fig. 10). The second value is in accordance with that previously calculated. For data representation a dot-map (with the diameter of dots proportional to gas content) were preferred instead of contour lines to emphasise the punctual data and to outline the presence of aligned anomalous values (*i.e.* the possible existence of fracture systems).

Figure 11 shows the dot-map of helium concentration in the Era basin. It defines:

– zones with helium contents close to atmospheric reference (negative to +130 ppb  $\Delta\text{He}$  values), where



Table 2 - Main statistics of helium in soil gas. Starred mean and standard deviation have been calculated by excluding values lower than 5th percentile and greater 95th percentile. The anomaly threshold was fixed at  $\text{mean}^* + 1/2$  standard deviation\*.

Tabella dei principali parametri statistici relativi al totale dei campioni prelevati. I valori della media e della deviazione standard contrassegnati dall'asterisco sono stati calcolati escludendo dal set di dati le concentrazioni inferiori al 5° percentile e quelle superiori al 95°. Il valore di soglia di anomalia è stato, quindi, calcolato sommando la media\* + 1/2 la deviazione standard\*.

	count	min	max	mean	std.dev.	5th%	95th%	mean*	std.dev.*	an. threshold
He (ppb)	919	-350	670	212	130	0	430	212	100	262

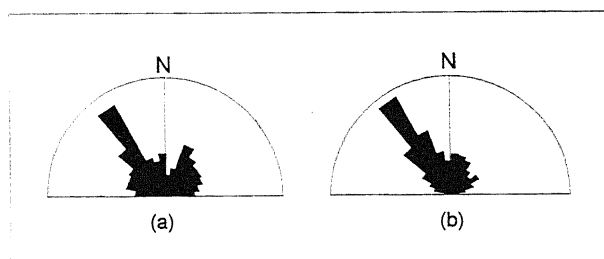


Fig. 7 - Rose diagrams serving to compare known faults (see Fig. 3) to photolineaments (see Fig. 6) in the Era river basin.

Diagrammi semipolari relativi alle faglie note (vedi Fig. 3) ed i lineamenti telerilevati (vedi Fig. 6).

deep-seated gases probably do not contribute because of a low primary and/or secondary permeability. Helium anomalies are frequently negative. Case histories show that this phenomenon also occurs in correspondence with gas-bearing faults (Reimer *et al.*, 1979a), a fact interpreted by some authors as being due to dilution in the presence of more abundant gas species (Reimer, 1980; Klusman, 1993). It is worth noting, however, that dilution is an unlikely mechanism for helium anomalies below -300 ppb. Perhaps a more convincing hypothesis is that negative helium anomalies are produced by near surface conditions (*i.e.* soil humidity and weathering) resulting in a local flux disequilibrium between soil gas and the atmosphere (Gregory & Durrance, 1985). In this case negative anomalies are usually formed when fractures are water-conducting, thus gas depletion occurs as a result of the low solubility of helium in water.

– zones characterised by high anomalies ( $\Delta\text{He} > 262$  ppb), which indicate the presence of deep-seated gases and where a helium flux can be inferred. Greater fracturing (fault and fracture systems) may be suggested for these areas, as they would act as preferential migration pathways for endogenetic gases.

In the map the possible alignments of helium anomalous values are also shown.

The majority of helium anomalous trends in some cases coincide with the known structural features (NW- and NE-trending faults); in particular they seem to be aligned with the recent tectonic structures bordering the basin (*i.e.* the western and the eastern ridges of the area). Linear helium trends also occur in the central part of the Era basin. These include the concentration values elongated N-S and E-W from Peccioli to Montecatini in Val di Cecina villages and from Casciana T. and Cedri villages. Furthermore, an important NW-SE helium trend crosses the basin: the presence of a similar trending structure is shown in Figure 3. Minor soil-gas alignments

trending NW-SE and NE-SW in the northern and western sector occur. In particular the inferred alignments N40°-50°W and N50°-60°E between the Montecatini and the Laiatico villages seem to coincide with the intense fracturing probably due to Plio-Quaternary trachyte intrusions suggesting a renewed extensional tectonics.

To better assess the presence of the previously recognised linear trend of helium concentrations, continuous lines were automatically drawn linking values greater than the anomaly threshold (Fig. 12). These lines are the graphic result of data treatment performed using an autocad-based software written in the autolisp language specifically for this type of study (Ciotoli *et al.*, unpubl. rep.). This statistical approach was aimed to refine criteria for defining the spatial distribution of anomalous gas concentrations aligned along gas-bearing fractures. It attempts to process unbiased criteria to define anomalies and to infer correlations on their fault-related linear geometry. Results shown in the map of Figure 12, generally, confirm the recognised linear pattern.

## 8. DISCUSSION

The prevailing alignments defined in the study area, using statistical analysis of rectilinear stream segments, geomorphological, meso-structural and geochemical data are NW-SE (Figs. 5, 7, 9, 11, 12), in agreement with the known Apennine structural trends. Moreover, the N-S and E-W orientations of helium anomalous concentrations (Figs. 11 and 12) suggest along these directions the presence of areas of enhanced permeability along which a deep-seated gas leakage occurs. These can be due to the existence of N-S and E-W fault and fracture systems linked to the recent tectonic activity, starting from Lower Pleistocene. The effect of the last tectonic phase are not yet recognisable by statistical analysis extended to the whole basin. Nevertheless, the inferred relationship between helium distribution and the strain field is strengthened by the good correspondence, at local scale, among geochemical data and the results of the structural and geomorphological features as below:

– Helium trends in the northeastern and western sides of the basin well agree with the NW-SE main tectonic lines that characterize the structural setting of the basin as reported in Figure 3. This trend is also observed, at local scale, from the fracture field (stations 22, 25, 26, 28, 29 and subordinately 31, 33, 48 in the western sector; 39, 41, 42, 44 and 45 in the northeastern sector);

– At regional scale the NW-SE linear helium trend crossing the basin coincides with the general structural

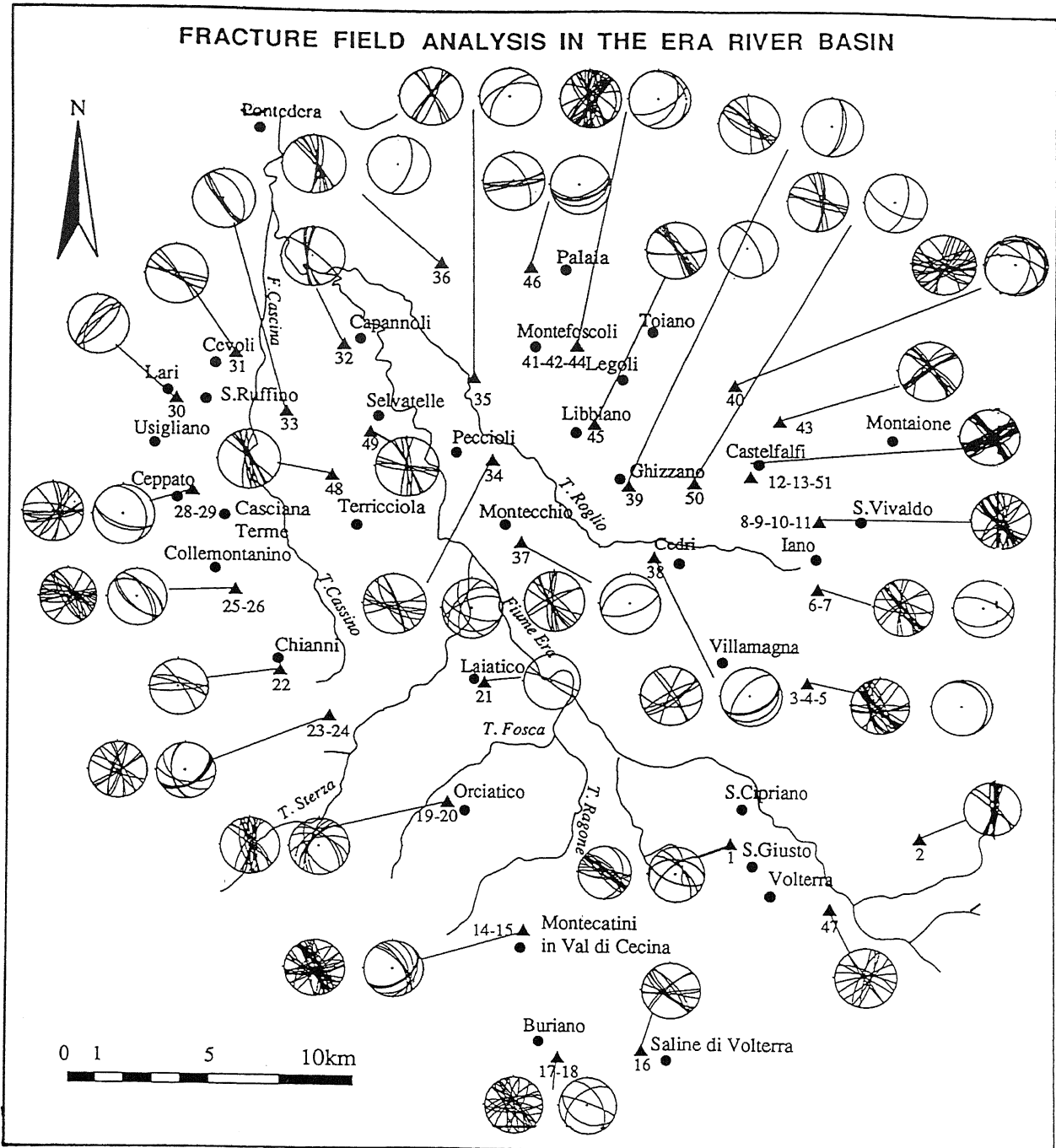


Fig. 8 - Fracture field analysis. The picture shows the location of mesostructural stations and the projection of fractures and fault planes on the Schmidt's net. For each station, the circle on the left is related to fractures, that on the right, if present, is related to faults.

*Analisi del campo di fratturazione. La figura mostra l'ubicazione delle stazioni di rilevamento mesostrutturale e le proiezioni dei piani di faglia e di frattura sul reticolo di Schmidt. Per ogni campione il reticolo di Schmidt di sinistra è relativo alle fratture, quello di sinistra, se presente, è relativo alle faglie.*

setting of the area as also evidenced from Figures 3, 5, 7 and 9.

– The highest helium anomalous values (up to 450 ppb) occur in the area between the Orciatice and Montecatini V.C. villages, and are oriented N-S, N50°W and N30°E. These trends are similar to those of the two N10°W and N55°W trending fault systems that are present in this zone (Fig. 3). In the same area these trends can also be observed from photo-lineaments (N10°-20°W near Montecatini V.C. and N50°-60°W near Orciatice)

(Fig. 6) and from fracture field analyses in the stations 20 and 19 (N10°-30°W) (Fig. 8). The drainage network also points out two peaks N30°-40°W and N40°-50°W showed in the rose diagrams related to Sterza river, Ragone river and Botro d'Alpino river (Fig. 4).

– In the northern sector of the basin the main linear anomalies trend E-W between the Casciana T. and Cedri villages, and N-S from Peccioli to Chianni villages. In the same zone the statistical analysis of brittle deformations shows similar trends (*i.e.* fracturing trends of the stations

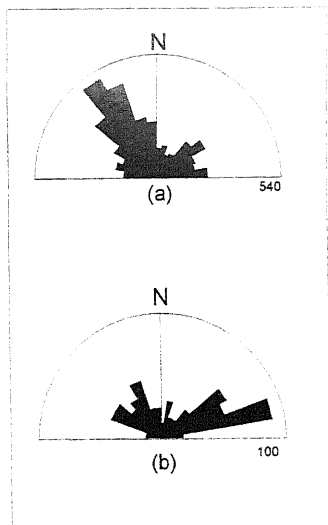


Fig. 9 - Rose diagram showing the distribution of the directions of all fractures (a) and faults (b) evidenced by the meso-structural survey in the Era river basin.

*Diagramma semipolare che mostra le direzioni delle fratture (a) e delle faglie (b) rilevate dall'analisi mesostrutturale nel bacino del Fiume Era.*

28, 32, 34, 36, 37, 42 and 49 vary from N5°-10°E to N10°-20°W). The same trends are confirmed by the statistical analysis of fluvial streams reported in the diagrams related to Casciana river (E-W and N-S) and Roglio river (N80°W) suggesting the close relation between helium anomalies and morpho-structural features. These two rivers show a clear and sharp deviation of their course.

In the whole, helium distribution in soil gas seems not to be affected by lithological changes except in the area near Montecatini V.C. and Orciatino where the out-

croppings of trachytic intrusions are marked by high helium values. These latter may be originated by a higher U content in volcanic rocks and/or by an enhanced deep-seated helium leakage through the fractured area causing the intrusions, as suggested by the local correspondence between the direction of helium anomaly axis and fault direction.

As aforesaid, the reconstruction of main helium anomaly trends (Fig. 11) may be affected by sampling density and by the different permeability of fracture systems due to different age of activation and/or self-sealing phenomena. Nevertheless the dominating NW-SE, N-S and subordinately E-W trends of helium anomalous concentrations (Figs. 11 and 12) indicate a clear enhanced gas permeability along these directions, and thus the presence of faults, even when clay fill may mask the surface expression of structural features.

## 9. CONCLUSIONS

The proposed method, based on the integration of geochemical, morphological and structural surveys yielded a more accurate reconstruction of the strain field of the investigated area. Results from statistical analysis of helium soil gas distribution, drainage pattern, photolineaments and brittle deformation are, consistent with the NW-SE orientations at regional scale, and with the NE-SW trends at local scale (*i.e.* Apennine and anti-

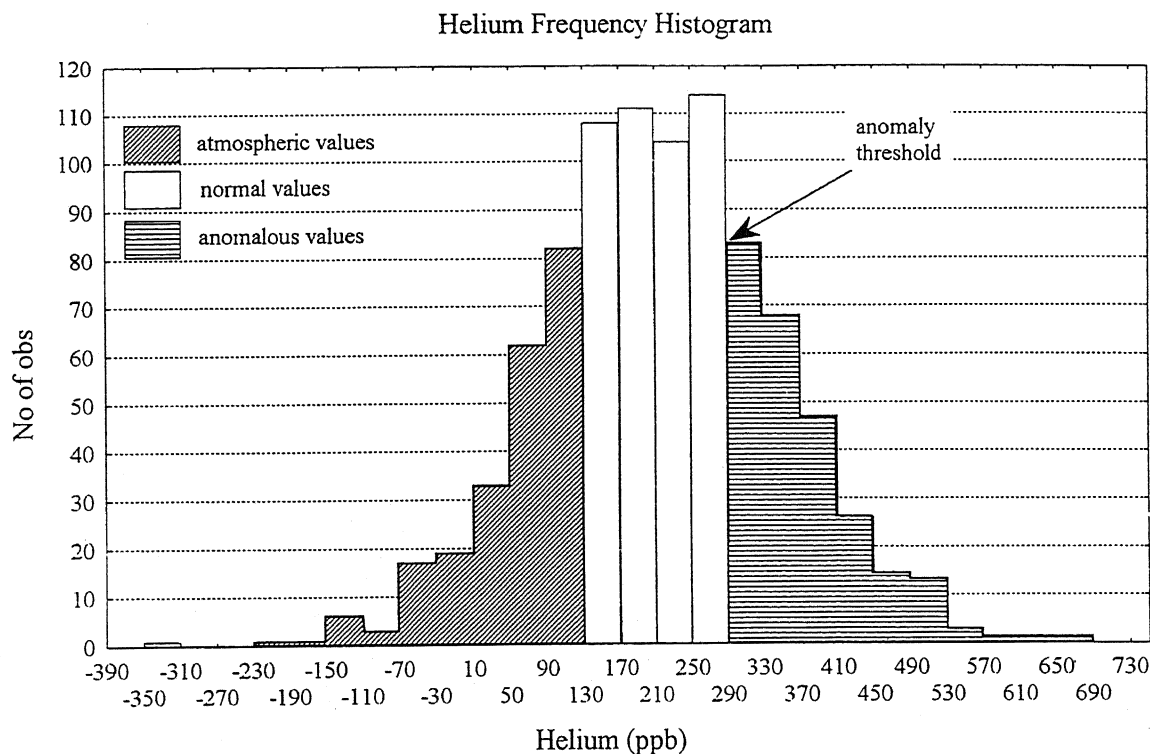


Fig. 10 - Helium frequency histogram. The steps in the frequency distribution histogram highlight the presence of two threshold values of 130 ppb and 290 ppb defining samples near the atmospheric helium content (negative to 130 ppb), the background concentrations (130 - 290 ppb) and the anomalous values (up to 290 ppb), respectively.

*Istogramma di frequenza relativo alle concentrazioni di elio nei gas del suolo. L'analisi delle frequenze delle concentrazioni di elio ha permesso il riconoscimento di tre classi di concentrazioni relative rispettivamente a valori atmosferici (fino a 130 ppb), valori di background (tra 130 e 290 ppb) e valori anomali (superiori a 290 ppb).*

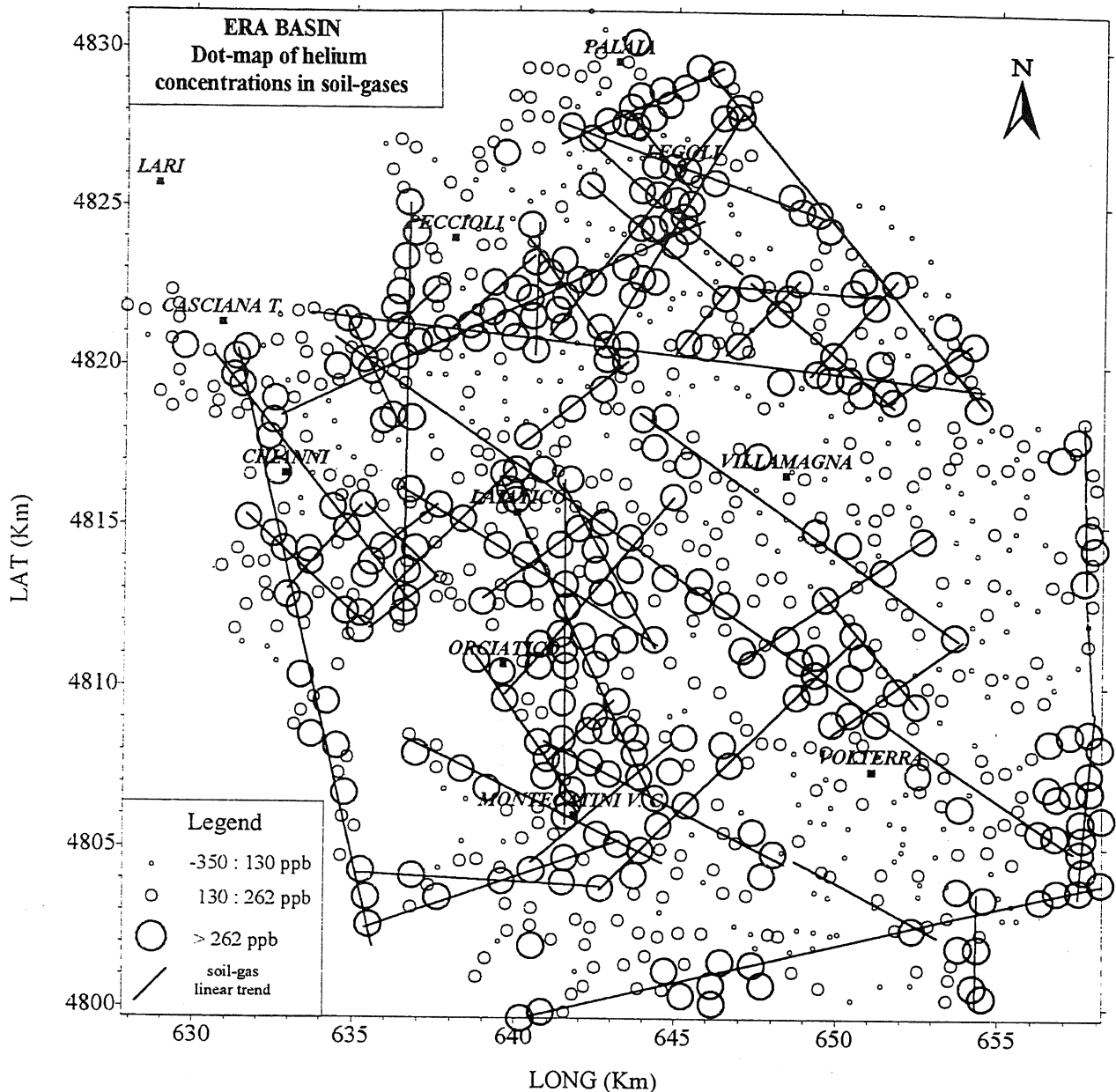


Fig. 11 - Dot map of helium distribution in soil gas. Diameter of dots is proportional to concentration values. The map shows zones with helium contents close to atmospheric reference (south and western sectors of the investigated area), where deep-seated gases probably do not contribute because of a low primary and/or secondary permeability, and where the negative helium anomalies are produced by near-surface conditions (*i.e.* soil humidity and weathering) resulting in a local flux disequilibrium between soil gas and the atmosphere. Zones characterised by high anomalies mainly elongated according to NW-SE, NE-SW, N-S and subordinately E-W, trends (northeastern sector and the area between Laiatico and Montecatini in Val di Cecina villages), where a helium flux can be inferred and a greater fracturing (fault and fracture systems) may be suggested, as they would act as preferential migration pathways for endogenous gases.

Dot-map delle concentrazioni di elio nei gas del suolo. La figura mostra la presenza di concentrazioni di elio riferibili allo standard di riferimento atmosferico (da valori negativi a 130 ppb). Tali concentrazioni (settori meridionale ed orientale dell'area investigata) si riferiscono a zone caratterizzate da una bassa permeabilità primaria/secondaria o dove l'influenza dei parametri atmosferici causa fenomeni di diluizione con altre specie gassose. Le aree corrispondenti ai settori settentrionale ed occidentale e la zona tra gli abitati di Laiatico e Montecatini in Val di Cecina sono caratterizzate, al contrario, dalla presenza di elevate concentrazioni di elio (superiori al valore di soglia calcolato, 290 ppb) allineate principalmente secondo le direzioni NW-SE e NE-SW, N-S e subordinatamente E-W. Tali allineamenti suggeriscono la presenza di sistemi di faglia e/o fratture che costituiscono le rapide vie di risalita per gas endogeni.

Apennine trend of the known structural pattern in the Era basin). In addition, N-S and E-W trending high helium values clearly mark the existence of enhanced gas permeability pathways along these directions. Deep-seated gas leakage towards the atmosphere is possibly linked

to the N-S and W-E fracture system related to the tectonic phase active during lower-middle Pleistocene whose effect are locally recognised but not on a statistical basis all around the basin. In fact the suggested structural control for helium leakage is confirmed by the

good correspondence, at local scale, between geochemical data and the results of brittle deformation and geomorphological analysis. Helium soil-gas technique showed to be a sensible tool for neotectonic studies in clay basin, as soil-gas defined the leakage of deep-seated gas along tectonic discontinuities even if they have no surface evidence and where the clay deposit is hundreds of meters thick.

## ACKNOWLEDGEMENTS

We are very grateful to Dr. S. Beaubien for the revision of the manuscript and his helpful suggestions. We wish to thank Mrs. A. Baccani for her help in the laboratory analyses. The research was performed in collaboration with ENEA and funded by the European Community under the Nuclear Fission & Safety Programme

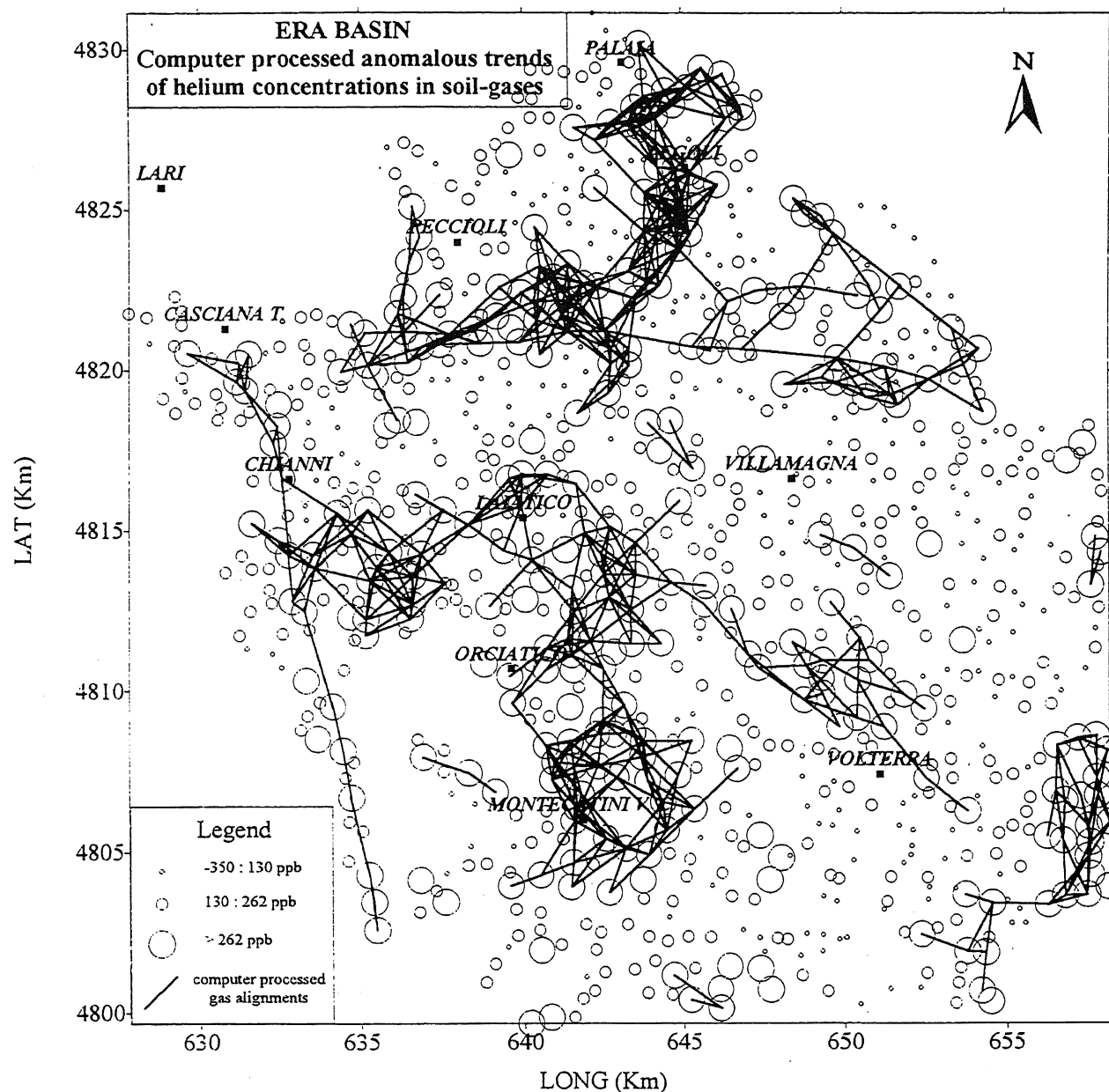


Fig. 12 - The figure shows an example of a moving window statistics which may be considered as the first step of a geostatistical analysis. Continuous lines represent the main anomalous trends and they link anomalous points. These lines are the graphic result of data treatment performed using an autocad-based software written in the autolisp language specifically for this type of study (Ciotoli *et al.*, unpublished). This statistical approach was aimed to refine criteria for defining the spatial distribution of anomalous gas concentrations aligned along gas-bearing fractures. It attempts to process unbiased criteria to define anomalies and to infer correlation on their fault-related linear geometry. Results shown in the figure confirm, at regional and local (in some cases) scale, the linear pattern recognised in Figure 11.

La figura mostra un esempio di elaborazione statistica con la tecnica del moving windows. Questo tipo di analisi statistica utilizzata nello studio della media e della variabilità acquista importanza soprattutto nelle procedure di stima di una variabile e rappresenta una delle tecniche di base utilizzate nella geostatistica. Le linee riportate in figura costituiscono il risultato grafico di un'elaborazione dei dati effettuata tramite un software scritto specificatamente per questo tipo di analisi in linguaggio Autolisp. Esso costituisce un metodo automatico per definire dei criteri di elaborazione dati utili al riconoscimento delle anomalie lineari e, quindi, ad un loro possibile legame con la geometria generalmente lineare degli elementi di tettonica fragile. I risultati confermano, a scala regionale, gli allineamenti riconosciuti in Figura 11.

## REFERENCES

- Al Fasatwi Y.A. & Van Dijk P.M., 1990 - *Lineament and geomorphic analysis remote sensing data as an aid to hydrocarbon exploration, Sirt Basin*. ITC Journal, **1990-2**, 137-144.
- Ambrosetti P., Carboni M.G., Costantini A., Esu D., Gandin A., Girotti O., Lazzarotto A., Mazzanti R., Nicosia U., Parisi G. & Sandrelli F., 1978 - *Evoluzione paleogeografica e tettonica nei bacini Tosco-umbro-laziali nel Pliocene e nel Pleistocene inferiore*. Mem. Soc. Geol. It., **19**, 573-580.
- Anderson E.M., 1951 - *The dynamics of faulting*. Oliver & Boyd, Edimburg.
- Atzori P., Ghisetti F., Pezzino A. & Vezzani L., 1978 - *Struttura ed evoluzione geodinamica recente dell'area Peloritana (Sicilia nord-orientale)*. Boll. Soc. Geol. It., **98**, 31-56.
- Bagheri S. & Kieffer R.W., 1986 - *Regional geologic mapping of digitally enhanced Landsat imagery in the southcentral Alborz mountain of Northern Iran*. In: Damen M.C.J., Sicco Smith G. & Verstappen H.Th. (Eds.), "Remote Sensing for Resources Development and Environmental Management". Vol 2, 555-559.
- Bartolini C., Bernini M., Carloni G.C., Costantini A., Federici P.R., Gasperi G., Lazzarotto A., Marchetti G., Mazzanti R., Papani G., Pranzini G., Rau A., Sandrelli F., Vercesi P.L., Castaldini D. & Francavilla F., 1982 - *Carta neotettonica dell'Appennino settentrionale. Note illustrative*. Boll. Soc. Geol. It., **101**, 523-549.
- Bemporad S., Conedera G., Dainelli P., Ercoli A. & Facibeni P., 1986 - *Landsat Imagery: a valuable tool for regional and structural geology*. Mem. Soc. Geol. It., **31**, 287-298.
- Bertagnini A., Carboni G., Ciccacci S., De Rita D., Di Filippo M., Faccenna C., Funiciello R., Landi., Sciacca P., Vannucci N. & Zarlenga F., 1991 - *Evoluzione geologico-petrografica dei Monti Ceriti*. Mem. Serv. descr. C. G. d'It., in press.
- Bertrami R., Ceccarelli A. & Lombardi S., 1984 - *L'elio nei gas del suolo nella prospezione geotermica*. Rend. Soc. It. Min. Petr., **39**, 331-349.
- Bisci C., Calamita F. & Dramis F., 1988 - *Analisi computerizzata della orientazione di tratti rettilinei di reticolo idrografico e implicazioni neotettoniche: un esempio nell'area umbro-marchigiana*. Suppl. Geogr. Fis. Dinam. Quat., **1**, 189-196.
- Boccaletti M., Ciaranfi N., Cosentino D., Deiana G., Galati R., Lentini F., Massari F., Moratti G., Pescatore T., Ricci Lucchi F. & Tortorici L., 1990 - *Palinspastic restoration and paleogeographic reconstruction of Theperi-Tyrrhenian area during the Neogene*. Palaeogeogr. Palaeoclim. Palaeoecol., **77**, 41-50.
- Boccaletti M. & Coli M., 1983 - *La tettonica della Toscana: assetto ed evoluzione*. Mem. Soc. Geol. It., **25**, 51-62.
- Boccaletti M., Coli M., Eva C., Ferrari G., Giglia G., Lazzarotto A., Morlanti F., Nicolich R., Papani G. & Postpischl D., 1985 - *Considerations on the seismotectonics of the Northern Apennines*. Tectonophysics, **117**, 7-38.
- Bollettinari G. & Mantovani F., 1986) - *Comparision between interpretation of images of different nature*. In: Damen M.C.J., Sicco Smith G. & Verstappen H.Th. (Eds.): "Remote sensing for resources Development and Environmental Management". Vol. 2, 569-571.
- Brancaccio L., Cinque A. & Sgrosso I., 1986 - *Elementi morfostrutturali ereditati nel paesaggio dell' Appennino Centromeridionale*. Mem. Soc. Geol. It., **35**, 869-874.
- Carraro F., Martinotti G. & Polino R., 1978 - *Lineamenti e faglie: analisi delle possibilità di corrispondenza fra i due fenomeni*. Gr. Strat. Quat. Pad., **4**.
- Castaldini D. & Panizza M, 1988 - *Contributo alla definizione del limite tra evidenze di neotettonica e fenomeni dovuti ad altre cause*. Suppl. Geogr. Fis. Dinam. Quat., **1**, 11-23.
- Ciccacci S., Fredi P., Lupia Palmieri E. & Salvini F., 1987 - *An approach to the quantitative analysis of the relations between drainage patterns and fracture trend*. Proc. 1st Int. Congr. Geom., **2**, 49- 68.
- Chorowicz J., Deroin J.P., Gess G., Huger J., Becue B., Curnelle R., Perrin G. & Ronfola D., 1991 - *A methodology for the use of SPOT imagery in oil exploration. Example of the Bas Languedoc exploration permits area (France)*. Int. J. Remote Sensing, **12**(10), 2087-2108.
- Ciotoli G., Etiopie G., Lombardi S., Naso G. & Tallini M., 1993 - *Geological and soil gas investigation for tectonics prospecting : preliminary results over the Val Roveto fault (Central Italy)*. Geologica Romana, **29**, 483-493.
- Cloos E., 1968 - *Experimental analysis of fracture patterns*. A.A.P.G. Bull., **52**, 420-444.
- Cosentino D., Gliozzi E. & Salvini F., 1987 - *Brittle deformations in the Upper Pleistocene deposits of the Crotona Peninsula (Calabria) Southern Italy*. Tectonophysics, **163**, 351-354.
- Dallan L., Raggi G., Squarci P., Taffi L. & Trevisan L., 1969 - *Note illustrative della C.G.I.- F. 112 (Vollterra)*. Serv. Geol. d'It.
- Danielska B.D., Kibitlewsky S. & Sadursky H., 1986 - *Geological analysis of the satellite lineaments of the Vistula Delta Plain, Zulawy Wislane, Poland*. In: Damen M.C.J., Sicco Smith G., Verstappen H.Th. (Eds.): "Remote Sensing for Resources Development and Environmental Management". Vol. 2, 579-584.
- Davis G.H., 1984 - *Structural geology of rocks and regions*. J. Wiley & Sons, New York.
- Davis J.C., 1986 - *Statistics and data analysis in geology*. J. Wiley & Sons, 2nd Ed., 645 pp.
- Defu L., Wenhua A., Bingguang L., Ruisong X. & Baolin G., 1986 - *Analysis of lineaments and major fractures in Xichang-Dukou area, Sichuan province as interpreted from Landsat images*. In: Damen M.C.J., Sicco Smith G., Verstappen H.Th. (Eds.): "Remote Sensing for Resources Development and Environmental Management". Vol. 2, 585-588.
- Durrance E.M. & Gregory R.G., 1988 - *Fracture mapping in clays: soil gas survey at Down Ampney, Gloucester-*

- shire. DOE Rep. N° DOE/RW/88081.
- Duddridge G.A., Grainger P., Grindrod P., Lombardi S., & Impey M. D., 1991 - *The refinement of soil gas analysis as a geological investigative technique. Annual progress report.* CEC Programme on Radioactive Waste Management. Disposal of Radioactive Waste: research to back-up the development of underground repositories (Part A, Task 4).
- Elsinga R. & Verstappen H.Th., 1989 - *SPOT for earthquake hazard zoning.* ITC Journal, **1898-1**, 21-26.
- Etiopio G., 1995 - *Migrazione e comportamento del "Geogas" in bacini argillosi.* Ph. D. Thesis, Dept. of Earth Sciences, Università "La Sapienza", Roma, Italy.
- Ferrara G., Leoni L., Sartori F. & Tonarini S., 1988 - *Sr content and Sr isotopic composition in contact metamorphosed argillaceous sediments (Orciatice, Tuscany, Central Italy): relation to fluid circulation.* Rend Soc. Min. Petrol., **40**, 111-124.
- Frezzotti M. & Giraudi C., 1986 - *Indagini nella piana del Fucino (Abruzzo) mediante l'utilizzo di immagini Landsat.* Mem. Soc. Geol. It., **35**, 881-886.
- Fridman A.I., 1990 - *Application of naturally occurring gases as geochemical pathfinders in prospecting for endogenetic deposits.* J. Geoch. Expl., **38**, 1-11.
- Galadini F. & Salvi S., 1990 - *Processamento di immagini Landsat per l'interpretazione strutturale in aree tettonicamente attive: un esempio del margine sud-occidentale della catena del Gran Sasso.* Il Quaternario, **3**, 15-22.
- Gregory R.C. & Durrance E.M., 1985 - *Helium, carbon dioxide and oxygen soil gases: small-scale variation over fractured ground.* J. Geoch. Expl., **24**, 29-49.
- Gruppo Geologia Spaziale del Settore Alpino, 1978 - *Studio dei lineamenti nelle immagini da satellite in un settore campione dell'arco alpino.* Boll. Geod. Sci. Aff., **37**, 1.
- Holland P.W. & Emerson D.E., 1990 - *The global helium-4 content of near-surface atmospheric air.* In: *Geochemistry of gaseous elements and compounds.* Teophr. Publ. S.A., Athens.
- Karpuz M.R., Roberts D., Olsen O., Gabrielsen R.H., & Herrevold T., 1993 - *Application of multiple data sets to structural studies on Varanger Peninsula, Northern Norway.* Int. J. Remote Sensing, **14**(5), 979-1003.
- Kibitlewski S. & Danielska B.D., 1986 - *Remote sensing methods in geological research of the Lublin coal basin, SE Poland.* In: Damen M.C.J., Sicco Smith G., Verstappen H.Th. (Eds.): *"Remote Sensing for Resources Development and Environmental Management"*. Vol. 2, 619-624.
- King C.Y., King B.S., Evans W.C. & Zang W., 1996 - *Spatial radon anomalies on active faults in California.* Appl. Geochemistry, **11**, 497-510.
- Klusman R.W., 1993 - *Soil gas and related methods for natural resource exploration.* J. Wiley & Sons, N.Y., 483 pp.
- Illing V.C., 1933 - *Migration of oil and natural gas.* Inst. Petroleum Technology J., **19**, 229-274.
- Le Corre C. & Quete Y., 1993 - *Tectonique et trajectoires de texture: méthode et tests sur des données SPOT dans la Chaîne Varisque Marocain.* Int. J. Remote Sensing, **14**(6), 1043-1054.
- Lepeltier C., 1969 - *A simplified statistical treatment of geochemical data by graphical representation.* Economic Geology, **64**, 538-550.
- Lombardi S. & Reimer G.M., 1990 - *Radon and Helium in soil gases in the Phlegrean Fields, Central Italy.* Geophys. Res. Lett., **17**, 849-852.
- Lombardi S., Benvegnù F., Brondi A. & Polizzano C., 1993 - *Field investigations with regard to the impermeability of clay formations: Helium-4 soil gas surveys in sedimentary basins as a tentative study of secondary permeability in clayey sequences. Final report.* Work carried out under contract with the European Atomic Energy Community in the framework of its shared cost R, D programme "Management and Storage of Radioactive Waste (1985-1989) Part A, Task 4 : "Geological disposal studies". EUR 14585 EN.
- Lombardi S., Etiopio G., Guerra M., Ciotoli G., Grainger P., Duddridge G.A., Gera F., Chiantore V., Pensieri R., Grindrod P. & Impey M., 1996 - *The refinement of soil gas analysis as a geological investigative technique. Final Report.* Work carried out under a cost sharing contract with the European Atomic Energy Community in the framework of its 4th R, D programme on "Management and Storage of Radioactive Waste" (1990-1994) Part A, Task 4: "Disposal of Radioactive Waste". EUR 16929 EN.
- Malmqvist L. & Kristiansson K., 1984 - *Experimental evidence for an ascending microflow of geogas in the ground.* Earth Planet. Sci. Lett., **70**, 407-416.
- Mazzanti R., 1961 - *Geologia della zona di Montaiione tra le Valli dell'Era e dell'Elsa (Toscana).* Boll. Soc. Geol. It., **80**, 37-126.
- Mazzanti R., 1983 - *Il punto sul Quaternario della fascia costiera e dell'Arcipelago di Toscana.* Boll. Soc. Geol. It., **102**, 419-556.
- Mazzanti R., Squarci P. & Taffi L., 1963 - *Geologia della zona di Montecatini Val di Cecina, in provincia di Pisa.* Boll. Soc. Geol. It., **82**, 1-68.
- McCarthy J.H. Jr. & Reimer G.M., 1986 - *Advances in soil gas geochemical exploration for natural resources: some current examples and practices.* J. Geophys. Res., **91**, 12327-12338.
- Muskat, 1946 - *The flow of homogeneous fluids through porous media.* J.W. Edwards Inc., Ann Arbor, Michigan.
- Nino F., Rivera L. & Angelopoulos A., 1993 - *Linear feature enhancing by hyperbolic-Gaussian filtering.* Int. J. Remote Sensing, **14**(14), 2617-2630.
- O'leary D.W., Freidman J.D. & Pohn H.A., 1976 - *Lineaments, linear, lineation: some proposed new standards for old terms.* Geol. Soc. Am. Bull., **87**, 1463-1469.
- Oliver B.M., Bradley J.G. & Farrar Iv H., 1984 - *Helium concentration in the Earth's lower atmosphere.* Geoch. et Cosmoch. Acta, **48**, 1759-1469.
- Panizza M., 1988 - *Geomorfologia Applicata.* NIS, Roma.
- Panizza M., Castaldini D., Bollettinari G., Carton A. & Mantovani F., 1987 - *Neotectonic research in applied geomorphological studies.* Zeit. Geom., **63**, 173-211.

- Panizza M. & Piacente S., 1978 - *Rapporti fra geomorfologia e neotettonica. Messa a punto concettuale*. Geogr. Fis. e Dinam. Quat., **1**, 138-140.
- Perotti C.R., Savazzi G. & Vercesi P.L., 1988 - *Evoluzione morfotettonica recente della zona compresa tra le testate del T. Nure e la Val d'Aveto*. Suppl. Geogr. Fis. e Dinam. Quat., **1**, 121-140.
- Pogorsky L.A. & Quirt G.S., 1981 - *Helium emanometry in exploring for hydrocarbons: part I*. In: *Unconventional methods in exploration for petroleum and natural gas II*. Southern Methodist Univ. Press., 124-135.
- Ragan D.M., 1967 - *"Structural Geology" an introduction to geometrical techniques*. J. Wiley & Sons, New York.
- Reimer G.M., 1980 - *Use of soil-gas helium concentrations for earthquake prediction: Limitation imposed by diurnal variation*. J. Geoph. Res., **85**, 3107-3114.
- Reimer G.M., 1990 - *Reconnaissance techniques for determining soil-gas radon concentrations: an example from Prince George County, Maryland*. Geophys. Res. Lett., **17**(6), 809-812.
- Salvini F. & Vittori E., 1982 - *Analisi strutturale della linea Olevano-Antronico-Posta (Ancona-Anzio Auct.): metodologie di studio delle deformazioni fragili e presentazione del tratto meridionale*. Mem. Soc. Geol. It., **24**, 337-355.
- Scheidegger A.E., 1980 - *The orientation of Valley trends in Ontario*. Zeit. für Geomorph., **24**, 19-30.
- Scheidegger A.E., 1981 - *The geotectonic stress field and crustal movements*. Tectonophysics, **71**, 217-226.
- Serafini S. & Vittori E., 1986 - *Risultati di uno studio statistico sulle mesostrutture della Val Roveto e dell'area di Sora (Lazio Meridionale)*. Mem. Soc. Geol. It., **35**, 631-646.
- Servizio Geologico d'Italia, 1965 - *Carta Geologica d'Italia. F.112 (Volterra)*. Serv. Geol. d'It., Roma.
- Squarci P. & Taffi L., 1963 - *Geologia della zona di Chianni-Laiatico-Orciatico (Provincia di Pisa)*. Boll. Soc. Geol. It., **82**, 219-291.
- Stearns D.W., Coyles G.D., Jamison W.R. & Morse J.D., 1981 - *Understanding faulting in the shallow crust. Contribution of selected experimental and theoretical studies*. In: *"Mechanical behaviour of crustal rocks"*. Amer. Geophys. Union, Geophys. Monographs, **24**.
- Vakin E.K. & Lyalin G.N., 1990 - *Soil gas anomalies and the detection of water-conduction zones within geothermal system*. In: *Geochemistry of gaseous elements and compounds*. Theophrastus Publ. S.A., Athens.
- Verstappen H.Th., 1983 - *Applied Geomorphology*. Geomorphological Surveys for Environmental Development. Elsevier, Amsterdam-Oxford-New York.
- Wakita H., Nakamura Y., Kita I., Fujii N. & Notsu K., 1980 - *Hydrogen release: new indicator of fault activity*. Science, **210**, 188-190.
- Wise D.U., Funicello R., Parotto M. & Salvini F., 1985 - *Topographic lineament swarms: Clues to their origin from domain analysis of Italy*. Geol. Soc. Am. Bull., **96**, 952-967.
- Zanchi A. & Tozzi M., 1987 - *Evoluzione paleogeografica e strutturale recente del Bacino del Fiume Albegna (Toscana meridionale)*. Geologica Romana, **26**, 305-325.
- Zarlenga F., 1985 - *Recent tectonics along the Bahr El Jebel (Witthe Nile) Valley, between Nimule and Juba (Southern Sudan)*. Boll. Soc. Geol. It., **107**, 1-11.
- Zhiguan S., 1991 - *A study on the origin of fault gases in Western Yunnan*. Earthquake Res. in China, **5**(1), 45-52.

Ms. ricevuto il: 15.10.1996  
 Inviato all'A. per la revisione il: 20.4.1997  
 Testo definitivo ricevuto il: 23.9.1997

Ms received: Oct. 15, 1996  
 Sent to the A. for a revision: April 20, 1997  
 Final text received: Sept. 23, 1997